Video-rate near-infrared optical tomography using spectrally encoded parallel light delivery

Daqing Piao, Shudong Jiang, Subhadra Srinivasan, Hamid Dehghani, and Brian W. Pogue

Thayer School of Engineering, Dartmouth College, Hanover, New Hampshire 03755

Received April 4, 2005; revised manuscript received May 13, 2005; accepted May 23, 2005

A novel parallel source implementation approach to near-infrared tomography is demonstrated through spectral encoding of the light delivery. This new technique allows many sources to be input into the tissue at the same time, and a high-resolution spectrometer is used to spatially spread out the signals from each spectrally encoded source. The parallel sampling of all sources at all detection locations renders rapid imaging. Acquisition of complete tomographic data sets at a video rate of 35 frames/s is achieved for imaging of a 6.35 mm diameter inclusion with an absorption coefficient of 0.01 mm^{-1} and a reduced scattering coefficient of 1.5 mm^{-1} that is moving along a circular path inside a 1% Intralipid solution. © 2005 Optical Society of America

OCIS codes: 170.6960, 170.3880, 170.3890, 170.6920.

It is widely accepted that near-infrared (NIR) measurements of the attenuation between blood and parenchymal tissue have considerably high contrast. Owing to the high degree of vascularity in tumors, there is an elevated hemoglobin content and hence high intrinsic optical contrast between tumor and normal tissues.[1–4] Since the functionality of the tumor vasculature is known to be different from that of normal tissue, time-resolved acquisition of functional changes in tissue could provide a fundamentally new way to image tumors. The notably high contrast of optical signals *in vivo* substantiates the principle that rapid measurements can be obtained for evaluating the temporal changes of blood volume and oxygenation in the circulation.[5] However, currently there is no NIR system that can tomographically image transient phenomena in deep tissue volumes faster than a few hundred milliseconds without gating or other time-sharing techniques. The difficulty of achieving rapid imaging in NIR tomography is due to the fact that the diffuse pattern of photon migration in biological tissue demands that each source–detector (S-D) pair be encoded properly and decoded afterward to get localized information. The most straightforward approach to encoding–decoding is mechanical switching of the S-D pairs, as demonstrated recently,[6] when full tomographic data sets were acquired at 3 Hz. Variations of this approach have been used by many groups, where signals from different S-D pairs are measured by use of parallel detection but with sequentially multiplexing of the source. The simplicity of this sequential approach ensures proper encoding; however, it ultimately requires a start–stop acquisition and a delay between source excitations, which will always require more time than a design in which all the sources can be delivered in parallel. In the frequency domain approach,[7] decoding of the S-D pairs can be performed after the signals from all channels reach the same detector; however, this multiplexing approach comes at a cost of linear reduction in the dynamic range. In the frequency domain approach there is also the inherent limitation that stronger signals overwhelm the signals from more distant sources, thereby causing a practical limit in the number of sources detected in parallel for a given S-D geometry.

In this Letter, a new technique of providing spatial source parallelization for rapid NIR tomographic measurements is demonstrated. In this novel approach, the sources are encoded spectrally by distributing their emission wavelengths in a narrow range, and the signals from simultaneously excited sources are separated spectrally by a high-resolution spectrometer prior to parallel detection with a CCD. The spectral bandgap of the sources is sufficient to allow separation by the spectrometer, yet the overall spectral bandwidth of the sources is small enough to provide effectively the same or near-uniform attenuation in tissues. This robust technique leads to parallel sampling of all sources at all detection locations, and thus a complete tomographic data set can be acquired in a single frame of CCD exposure. Complete decoding of all S-D pairs prior to detection renders rapid imaging by use of CCD and preserves each signal's dynamic range. In this Letter, video-rate NIR tomography at 35 Hz in data acquisition is demonstrated, which is believed to be the highest NIR tomography acquisition speed to date.

The custom-made spectrally encoded video-rate NIR tomography system is shown schematically in Fig. 1 with a photograph included as an inset. The system consists of eight laser diodes (LDs) for excitation through individual fibers, eight detection fibers, a high-resolution spectrometer (300 mm focal length and a holographic grating of 1200 lines/mm, Acton Instruments), a high-frame-rate CCD (512 $\times$ 512 pixel size, Cascade 512F, Roper Scientific), and a computer for data acquisition, processing, and image reconstruction. The key feature of this system is to decode the spectrally encoded signals from different sources prior to parallel detection by use of a high-resolution spectrometer coupled to the CCD detector. The LD sources were spectrally encoded simply and effectively by use of a number of single-mode lasers manufactured for the same spectral band whose emission wavelengths were varied slightly by adjusting the operating temperature (the typical tuning sensitivity of commercial LDs is 0.1–0.3 nm/°C).

0146-9592/05/192593-3/$15.00 © 2005 Optical Society of America

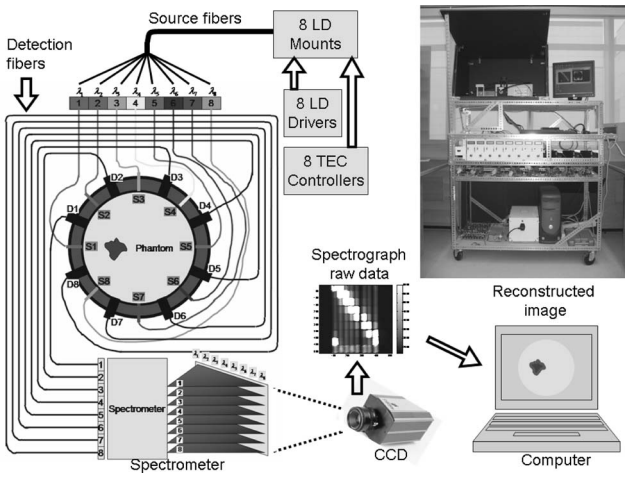

Fig. 1. Schematic diagram of the NIR tomography system by spectrally encoded parallel source delivery. The inset shows the photograph in which the bottom level on the cart is the power supply unit and computer, the middle level is the 8-channel LD source unit, and the top level is the detector unit consisting of an imaging fiber array, a spectrometer, and a CCD that are all enclosed in a light-tight hood.

The eight LDs had an emission wavelength between 777.8 and 786.5 nm, with 50 mW nominal output power. Each LD together with its mount was driven by an individual board-level constant-current driver and a thermal-electric cooling controller (both from Thorlabs). The temperatures and currents were set to provide a nearly even wavelength spacing, as shown in the measurement data of Fig. 2(a), where the intensity as a function of spectrum is shown for all eight lasers.

The laser emissions were focused onto individual SMA-terminated 600 μm fibers that were polished at the tissue contact end and arranged in a circular tomographic geometry. The detection fibers were also positioned in the same geometry interspersed between every two source fibers. The detection fibers were bare 800 μm cores enclosed in light-tight sleeves, and these fibers were aligned vertically at the spectrometer end to match the entrance slit. The detector locations were vertically separated, whereas the signals collected by each detector fiber coming from all the spectrally encoded sources were decoded horizontally. The result of spectral decoding of the sources combined with vertical spatial separation of detectors was a two-dimensional intensity map corresponding to all S-D pairs. The acquired time-series intensity maps were then transferred frame by frame in real time with video streaming software (StreamPix, Norpix) to the hard disk for later image processing, followed by tomographic image reconstruction and display.

A frame of this intensity map is shown in Fig. 2(b). The eight vertical columns left to right correspond to the signals from sources 1 to 8. Within each column, the eight rectangular blocks top to bottom represent detectors 1 through 8. This single frame of exposure provides a complete data set of 64 S-D pairs. The bottom row marked Ref is an extra channel used to monitor the emission stability of the eight lasers by collecting a small amount of light from each LD with individual 100 μm fibers.

In this system, the wavelengths of the eight lasers were separated by 1.25 nm on average, covering a total of 8.75 nm bandwidth. The diameter of the imaging tomography array was 27 mm, as specifically designed for imaging small animals. A tissue-simulating phantom of 27 mm diameter with an absorption coefficient of 0.006 mm^{-1} and a reduced scattering coefficient of 1.2 mm^{-1} was used for calibration of the system. It was found that 10 mW from each laser provided a sufficient signal for an exposure time of 5 ms/frame using an entrance-slit width of 125 μm. The dynamic range of detection is bounded by the 16-bit CCD (48 dB), and the cross talk is below the background streak level at this parameter setting. The data acquisition speed of 35 Hz provided acceptable data quality by binning the pix-

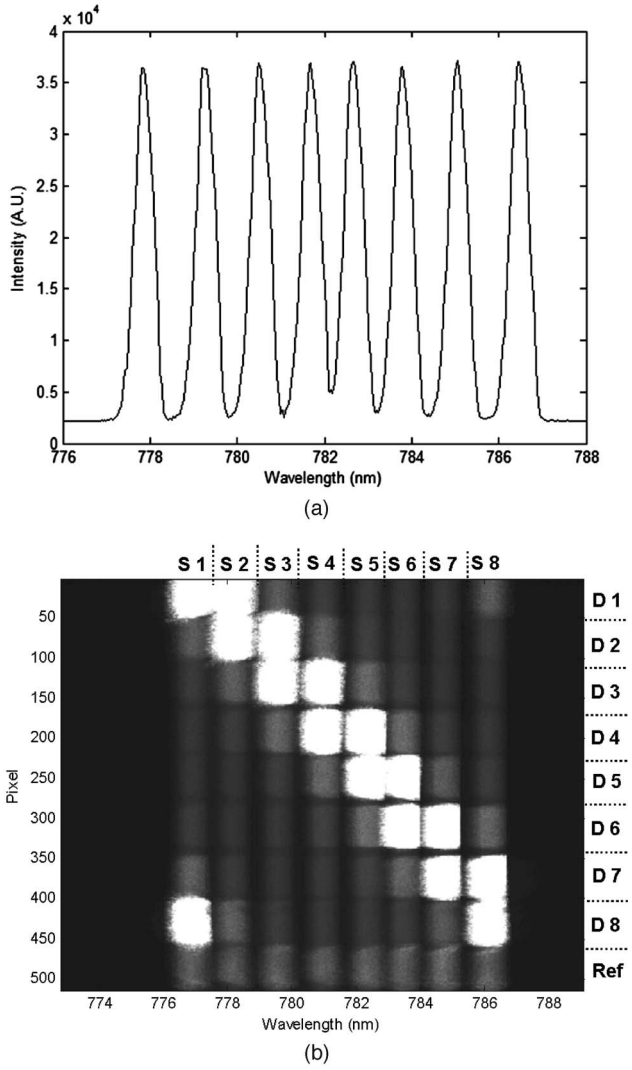

Fig. 2. (a) Emission profile of eight spectrally encoded LDs. (b) One frame of the acquired 2D data from the CCD. Markers S1–S8 at the top stand for sources 1–8, and markers D1–D8 on the right side indicate detection fibers 1–8. The label Ref at the right represents the reference sampling from all sources. Note that the gray scale has been set to show low-intensity signals, and thus the highest intensity signal shows up as saturated but actually is not.

els in 2 along the vertical dimension. After each frame was acquired and transferred to the hard disk, the signals corresponding to each of the 64 S-D pairs were averaged, and the resulting 8×8 intensity map was corrected by a calibration matrix that was determined with a known homogeneous phantom to compensate for the systematic coupling nonuniformity from the source fiber up to the CCD detector plane. The corrected 8×8 data matrix was then reshaped to 64×1 format to be used in the diffuse optical tomography reconstruction program that had been developed in earlier studies.[8] The object being imaged was a 6.35 mm diameter cylindrical phantom with an absorption coefficient of 0.01 mm^{-1} and reduced scattering coefficient of 1.5 mm^{-1} that was immersed in a 1% Intralipid solution, giving an absorption coefficient of 0.002 mm^{-1} and a reduced scattering coefficient of 1.0 mm^{-1}. The solution was held by a thin-walled (1 mm) container that fits exactly inside the imaging array. The phantom cylinder was attached to the rotor of a motor by a thin sewing wire, and it was driven clockwise along the inner surface of the container wall. The revolution speed of the phantom was slightly higher than 1 Hz, and therefore one complete revolution of the phantom resulted in nearly 35 images. Shown in Fig. 3 are these images with frames 1, 6, 11, 16, 21, 26, 31, and 36 displayed. The mean peak value of the phantom absorption coefficient for 35 consecutive frames was 0.0085 mm^{-1} with a standard deviation of 0.0014 mm^{-1}. This mean peak value corresponds to an accuracy of 15%. However, only the absorption coefficient was reconstructed due to the lack of phase information in the acquired data.[9]

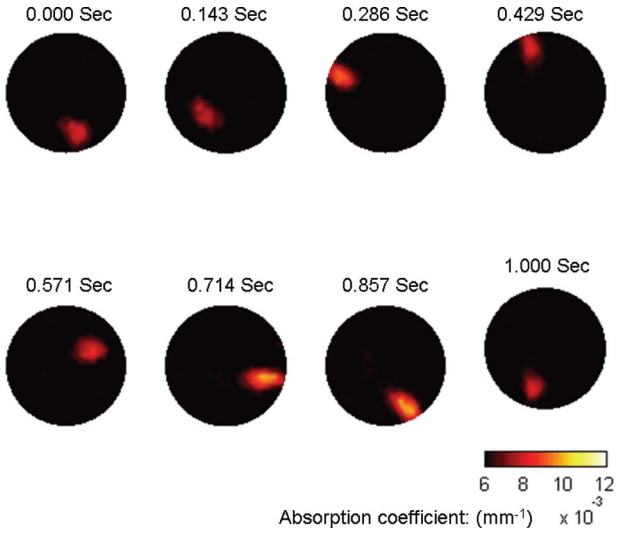

Fig. 3. Example of the images taken with a frame rate of 35 Hz. The four images in the top row are the frame series of 1, 6, 11, and 16, and the four images in the bottom row are the frame series of 21, 26, 31, and 36. The number at the top of each image shows the timing of each frame relative to the first one. Since the cylinder phantom immersed in the background Intralipid solution is revolving at a speed of slightly higher than 1 revolution per second, 35 consecutive frames should cover a complete revolution of the moving object. The true value of the absorption coefficient of the phantom is 0.01 mm^{-1}.

Although the data acquisition was performed at video rate, image reconstruction was handled off line by a nonlinear iterative approach with a speed of 10 s/frame for approximately ten iterations based on a Pentium IV 2 GHz CPU. Methodologies for real-time image reconstruction have been demonstrated[10] and can be readily implemented here with a single step of the Newton algorithm using a precalculated Jacobian and preinverted Hessian matrix. This approach will be attempted in the next phase of development of this system.

In summary, a new technique that provides spatial source parallelization in optical tomography measurements has been demonstrated. This technique implements source spectral encoding and spectral decoding of the signal by a spectrometer prior to CCD detection. The design allows simultaneous and rapid acquisition of signals from all S-D locations in parallel. Video-rate acquisition at 35 frames/s has been achieved. In future work, the system will be extended to include more wavelength bands that would render the potential of imaging changes in hemoglobin and oxygen saturation simultaneously.

The authors acknowledge the funding support by National Institutes of Health through grant 1R21CA100984-01A1 and resources from grant PO1CA80139. The authors thank Roger Springett, Peter Fontaine, Phaneendra K. Yalavarthy, and Xiaomei Song for helping with instrumentation and reconstruction. Correspondence can be addressed to Daqing Piao (daqing.piao@dartmouth.edu) or Brian W. Pogue (Pogue@dartmouth.edu).

References

1. B. Chance, Q. Luo, S. Nioka, D. C. Alsop, and J. A. Detre, Philos. Trans. R. Soc. London, Ser. B **352**, 707 (1997).
2. M. A. Franceschini, K. T. Moesta, S. Fantini, G. Gaida, E. Gratton, H. Jess, W. W. Mantulin, M. Seeber, P. M. Schlag, and M. Kaschke, Proc. Natl. Acad. Sci. U.S.A. **94**, 6468 (1997).
3. B. J. Tromberg, O. Coquoz, J. B. Fishkin, T. Pham, E. R. Anderson, J. Butler, M. Cahn, J. D. Gross, V. Venugopalan, and D. Pham, Philos. Trans. R. Soc. London Ser. B **352**, 661 (1997).
4. B. W. Pogue, S. P. Poplack, T. O. McBride, W. A. Wells, K. S. Osterman, U. L. Osterberg, and K. D. Paulsen, Radiology **218**, 261 (2001).
5. C. Nolte, M. Kohl, U. Scholz, M. Weih, and A. Villringer, Adv. Exp. Med. Biol. **454**, 115 (1998).
6. C. H. Schmitz, M. Löcker, J. M. Lasker, A. H. Hielscher, and R. L. Barbour, Rev. Sci. Instrum. **73**, 429 (2002).
7. S. Fantini, M. A. Franceschini, G. Gaida, E. Gratton, H. Jess, W. W. Mantulin, K. T. Moesta, P. M. Schlag, and M. Kaschke, Med. Phys. **23**, 149 (1996).
8. H. Dehghani, B. Brooksby, K. Vishwanath, B. W. Pogue, and K. D. Paulsen, Phys. Med. Biol. **48**, 2713 (2003).
9. Interested readers are directed to the following URL for examples of the reconstructed images: http://www-nml.thayer.dartmouth.edu/nir/downloads/Rubber_ball_movie_35fps_001.avi.
10. Y. Pei, H. L. Graber, and R. L. Barbour, in Proc. SPIE **4955**, 236 (2003).